

Toshiaki Kamitani
Yoshiyuki Kuroiwa
Lihong Wang
Mei Li
Yume Suzuki
Tatsuya Takahashi
Tadashi Ikegami
Sho Matsubara

Visual event-related potential changes in two subtypes of multiple system atrophy, MSA-C and MSA-P

Abstract We investigated the visual event-related potentials (ERPs) in two subtypes of multiple system atrophy (MSA) in 15 MSA-C patients, 12 MSA-P patients, and 21 normal control (NC) subjects.

Received: 28 August 2001
Received in revised form: 22 January 2002
Accepted: 25 January 2002

T. Kamitani · Y. Kuroiwa (✉) · L. Wang ·
M. Li · Y. Suzuki · T. Takahashi
Department of Neurology
Yokohama City University School
of Medicine
3-9, Fukuura, Kanazawa-ku
Yokohama, Japan
Tel.: +81-45/787 28 00
Fax: +81-45/788 60 41
E-Mail: ykuroiwa@med.yokohama-cu.ac.jp

T. Ikegami · S. Matsubara
Department of Radiology
Yokohama City University School
of Medicine
3-9, Fukuura, Kanazawa-ku
Yokohama, Japan

We used a visual oddball task to elicit ERPs. No significant changes were seen in N1 or N2 latency, in either MSA-C or MSA-P, compared with the NC group. An early stage of visual information process related to N1 and a visual discrimination process related to N2 might be preserved in both MSA-C and MSA-P. The P3a peak was more frequently undetectable in MSA than in the NC group. Significant P3a amplitude reduction in both MSA-C and MSA-P suggests impairment of the automatic cognitive processing in both MSA-C and MSA-P. Significant difference was found in P3b latency and P3b amplitude only in MSA-C, compared with the NC group. The result suggests the impairment of the controlled cognitive processing after the visual discrimination process in the MSA-C group. We further investigated the correlation between visual ERP changes and magnetic resonance

imaging (MRI) data. Quantitative MRI measurements showed reduced size of the pons, cerebellum, perisylvian cerebral area, and deep cerebral gray matter in both MSA-C and MSA-P, and of the corpus callosum only in MSA-P, as compared to NC group. In both MSA-C and MSA-P, P3b latency was significantly correlated with the size on MRI of the pons and the cerebellum. P3b latency in the whole MSA group was also significantly correlated with the size of the pons and the cerebellum. These results indicate that P3b latency changes in parallel with the volume of the pons and the cerebellum in both MSA-C and MSA-P.

Key words multiple system atrophy · visual event-related potentials · oddball paradigm · cognitive functions · quantitative MRI measurements

Introduction

The term multiple system atrophy (MSA) was first proposed in 1969 for three different entities, olivopontocerebellar atrophy (OPCA), striatonigral degeneration (SND), and Shy-Drager syndrome. According to the diagnostic criteria proposed by the Minneapolis Consensus Conference on MSA [3], MSA patients are divided into patients with predominant cerebellar features (MSA-C) and patients with predominant parkinsonian

features (MSA-P). Although cognitive dysfunction was not considered a main feature of MSA [1, 21], Wenning et al. reported that mental disturbance in pathologically proven MSA patients was relatively common; mild in 22 %, moderate in 2 %, and severe in 0.5 % [28]. The SND group, when compared with an age and IQ matched normal control group, showed abnormal results on neuropsychological tests sensitive to frontal lobe dysfunction [21, 22]. The SND group, when compared with a MMSE score-matched parkinson's disease group, showed significant deficits in attention tasks [11]. How-

ever, it is still not certain whether SND patients have deficits in global intelligence. Hirono et al. showed mild abnormalities in Wechsler Adult Intelligence Scale test, verbal fluency, visuospatial function, and depression scale in patients with spinocerebellar degeneration including OPCA [6]. They hypothesized that frontal lobe dysfunction exists in spinocerebellar degeneration with impaired cerebello-cerebral interconnections. From these neuropsychological studies, we can assume that the occurrence of mild cognitive deficits in MSA is not uncommon.

Many neurophysiological studies have used event-related potentials (ERPs) to evaluate cognitive impairments in neurodegenerative diseases. The ERPs during an oddball task can be regarded as an electrophysiological index of cognitive function. P3a after rare nontargets and P3b after rare targets reflect automatic and controlled cognitive processing, respectively [10, 30]. Recent reports [16, 27] indicate that neuropsychological evaluation may contribute to the differential diagnosis of movement disorders including MSA. Therefore, ERP testing may also assist in the differential diagnosis of MSA.

There are only a few previous ERP studies on MSA, and these reported the results from a small number of OPCA or SND patients [12, 26]. Our present study investigated statistical abnormalities of visual oddball ERPs in MSA-C and MSA-P. We also examined the morphological changes of the brain in MSA-C and MSA-P, by quantitative magnetic resonance imaging (MRI) measurements, and investigated the correlation between visual ERP changes and MRI data.

Subjects and Methods

Subjects

Diagnosis of MSA was determined on the basis of neurological examination as well as history of present illness and sporadic features of family histories. All patients were diagnosed as probable MSA on the basis of the diagnostic criteria for MSA proposed by the Minneapolis Consensus Conference [3]. Any patient with cerebral infarctions on MRI was excluded from the study. We investigated the patients diagnosed as MSA in Neurology Service, Yokohama City University Hospital, through 1996 to 2000. From these MSA patients, we only enrolled subjects who could still perform a visual oddball task. The MSA patients consisted of 15 MSA-C patients (7 men and 8 women) and 12 MSA-P patients (6 men and 6 women). The age of the MSA-C group ranged from 46 to 77 years, with a mean (standard deviation, SD) of 61.5 (9.2), and the age of the MSA-P group ranged from 49 to 74 years, with a mean (SD) of 62.3 (7.3). The normal control (NC) group consisted of 21 elderly healthy volunteers (9 men and 12 women) who were age-matched to the MSA-C and MSA-P patients. All the NC subjects showed normal neurological findings and had no specific neurological diseases. None of the NC subjects had any history of medical or psychiatric disorders or any abnormal MRI findings. The age of the NC group ranged from 48 to 77 years, with a mean (SD) of 61.6 (9.0).

The duration of illness and the clinical motor severity scores in

MSA-C and MSA-P patients are shown in Table 1. The onset age was defined as the age at which the patients first noticed neurological symptoms. The duration of illness in the MSA-C group ranged from 1 to 9 years, with a mean (SD) of 3.7 (2.6), and that in the MSA-P group ranged from 1 to 8 years, with a mean (SD) of 3.3 (2.0). The clinical motor severity scores in the patients were classified into 5 grades [5]: Grade 1, patients who did not need any assistance in walking; Grade 2, patients who needed assistance only when trying to stand, turn, and step up or down; Grade 3, patients who needed assistance in walking; Grade 4, patients who were unable to walk and needed assistance in standing; and Grade 5, bedridden patients. The clinical motor severity scores in the MSA-C group ranged from Grade 1 to Grade 5, with a mean (SD) of 2.47 (1.1), and those in the MSA-P group ranged from Grade 1 to Grade 5, with a mean (SD) of 2.33 (1.5).

On the Wechsler Adult Intelligence Scale-Revised (WAIS-R) test in MSA-C, the full-scale IQ ranged from 71 to 102 with a mean (SD) of 89.0 (11.4), verbal IQ ranged from 69 to 107 with a mean (SD) of 93.2 (15.6), and performance IQ ranged from 76 to 96 with a mean (SD) of 85.2 (8.8). On the WAIS-R test in MSA-P, the full-scale IQ ranged from 81 to 105 with a mean (SD) of 92.0 (10.8), verbal IQ ranged from 86 to 113 with a mean (SD) of 98.2 (11.0), and performance IQ ranged from 76 to 103 with a mean (SD) of 89.4 (12.1). We also performed the Hasegawa Dementia Scale-Revised test (full score, 30; demented, < 20), which has been widely used in several epidemiological studies in Japan [4]. The scores in MSA-C patients ranged from 23 to 30 with a mean (SD) of 27.1 (2.6), and the scores in MSA-P patients ranged from 21 to 30 with a mean (SD) of 27.3 (3.3).

As shown in Table 1, MRI data in our patients revealed the following abnormalities: slit-like signal changes at the posterolateral putamenal margin, cruciform signal changes in the pons (the "cross sign"), and atrophy in the pons and the cerebellum.

All subjects gave informed consent, as approved by the Ethical Committee of Yokohama City University School of Medicine.

Visual ERPs

A modified visual oddball task was used to elicit ERPs in MSA-C, MSA-P, and NC subjects. In the modified oddball task, three kinds of stimuli [rare target (20%), rare nontarget (20%), and frequent nontarget figures (60%)] were presented randomly on an electronic tachistoscope screen (Iwasaki Correspondence Company, Tokyo). The duration of each figure presentation was 68 ms. The interval between the onset of each sequential stimulus was 1600 ms (Fig. 1). Subjects were instructed to press the button with their right thumb only for rare target stimuli, as rapidly and correctly as possible.

Recordings were made using an evoked-potential analyser "Neuropack-8" (Nihonkoden), while the subjects were sitting comfortably in a silent and partially darkened room. The signals were recorded at scalp electrode sites Cz, Pz, and Oz (10–20 International System) using Ag/AgCl electrodes, referred to linked earlobes (A1/A2) with a forehead ground. The electrooculogram was monitored with a forehead-temple montage at a rejection level of $\pm 100 \mu\text{V}$. The inter-electrode resistance, checked before and after each recording session, was maintained below 5 k Ω . Bandwidth of the preamplifiers was 0.1 to 50 Hz. The EEG activity was analysed 100 ms preceding and 900 ms following each visual presentation. We recorded upward deflection of the electrical potentials as positive activity. Two trials of 10–20 summations to rare target stimuli were performed for each session, to confirm the reliability of recording.

N1 was identified after rare targets and rare nontargets as a negative component at Oz, occurring between 80 and 180 ms after the stimulus onset. N2 was identified as a negative component occurring between 200 and 400 ms after the stimulus onset. N2 was measured at Pz after rare targets and at Cz after rare nontargets, respectively. The P3 component was identified as the largest positive wave between 300 and 700 ms after the stimulus onset. P3a was defined as the P3 potential measured at Cz after rare nontargets. P3b was defined as the P3 potential measured at Pz after rare targets. Peak latencies for N1, N2,

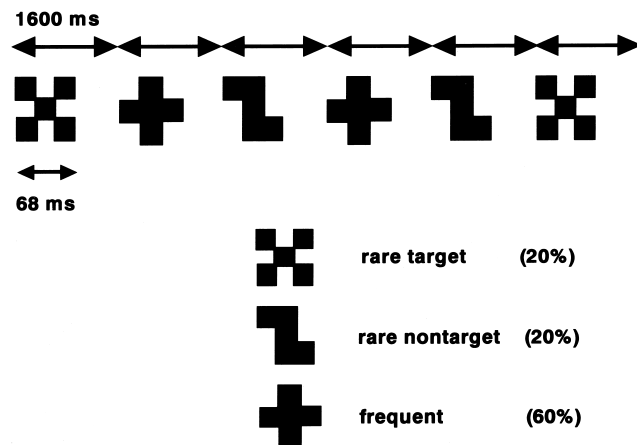
Table 1 Age, sex, duration of illness, clinical severity scores, and MRI findings in 15 MSA-C and 12 MSA-P patients

patient no.	age (years) and sex	subtype	duration of illness (years)	clinical severity scores	putamen		pons			cerebellum
					T2 (LI)	PR (HI)	T2 (HI)	PR (HI)	T1 (atrophy)	T1 (atrophy)
1	46 M	MSA-C	1	2	-	-	+	++	+	+
2	58 F	MSA-C	1	3	+	-	-	++	++	++
3	77 M	MSA-C	1	3	+	-	-	+	+	+
4	49 M	MSA-C	2	1	+	-	-	++	+	+
5	53 F	MSA-C	2	1	-	-	+	+	+	+
6	62 M	MSA-C	2	2	-	-	+	++	++	++
7	62 F	MSA-C	2	1	-	-	+	+	+	+
8	67 F	MSA-C	2	2	-	-	++	++	++	++
9	71 F	MSA-C	2	2	++	++	++	++	++	++
10	56 M	MSA-C	3	3	+	+	+	+	++	+
11	62 F	MSA-C	5	3	+	-	+	++	++	++
12	53 M	MSA-C	7	4	-	-	++	++	++	++
13	67 F	MSA-C	7	3	++	++	++	++	++	++
14	76 F	MSA-C	7	5	+	+	++	+	++	++
15	63 M	MSA-C	9	2	-	-	+	++	++	++
16	64 M	MSA-P	1	1	-	-	-	+	-	-
17	49 F	MSA-P	2	2	+	+	-	+	-	++
18	59 F	MSA-P	2	1	+	+	+	++	-	+
19	62 F	MSA-P	2	2	++	+	-	-	-	-
20	67 M	MSA-P	2	4	+	-	-	+	+	+
21	68 M	MSA-P	2	1	++	+	+	-	-	+
22	67 F	MSA-P	3	1	+	+	+	++	-	-
23	74 F	MSA-P	3	1	+	-	-	-	-	+
24	56 M	MSA-P	4	2	++	++	-	+	+	+
25	60 M	MSA-P	4	4	++	++	-	++	++	++
26	53 F	MSA-P	6	4	++	++	-	+	++	++
27	69 M	MSA-P	8	5	++	++	+	++	++	++

M = male, F = female

T1 T1 weighted images; T2 T2 weighted images; PR proton weighted images; (LI) low intensity MRI lesions; (HI) high intensity MRI lesions; putamen (LI/HI) MRI lesions in the posterolateral putamen; pons (HI) cruciform signal changes in the pons (the "cross sign")

+ moderate; ++ distinct; - absent

**Fig. 1** A sketch representing the time course and the task for a visual oddball paradigm

P3a, and P3b were measured as the interval between the stimulus onset and each peak. The peak latencies were not measured in trials where the peak could not be clearly recognized. The P3a and P3b amplitudes were defined as the amplitude difference between the P3a and P3b peaks and the prestimulus baseline. When the P3 peaks could

not be clearly determined, the peak amplitudes were arbitrarily defined as the maximum upward deflection in μV from the prestimulus baseline, during the period between 300 and 700 ms after the stimulus. Reaction time was defined as the mean interval between the onset of a rare target stimulus and the subject's button press.

Quantitative MRI measurements

MRI was performed with a 1.5-T MRI scanner (Signa, General Electric, Milwaukee, WI, USA) in MSA-C, MSA-P and NC subjects. The planes of sectioning in axial images were parallel to the AC-PC line (anterior commissure - posterior commissure line). Section thickness of the axial plane was 10 mm and that of the sagittal plane was 5 mm. Quantification of brain MRI morphology was carried out from axial and sagittal T1-weighted images (T1WI: echo time, 15 ms; repetition time, 500 ms). Four T1WI slices were chosen for quantitative square MRI measurements, and consisted of three axial slices (A, B, C) and one midsagittal slice (D), as shown in Fig. 2. Slice A was through the upper portion of the lateral ventricles. Slice B was through the basal ganglia and the thalamus. Slice C was through the middle cerebellar peduncle. NIH Image version 1.62 was used for automated MRI measurements. The anatomical boundaries between the brain tissue and the cerebrospinal fluid were defined as the points with mean signal intensities between the brain tissue and the cerebrospinal fluid. The ventricular areas were excluded from the measurements. We examined the square measurements of eleven brain regions, as shown in Fig. 2: (1) upper cerebral area in slice A, (2) anterior

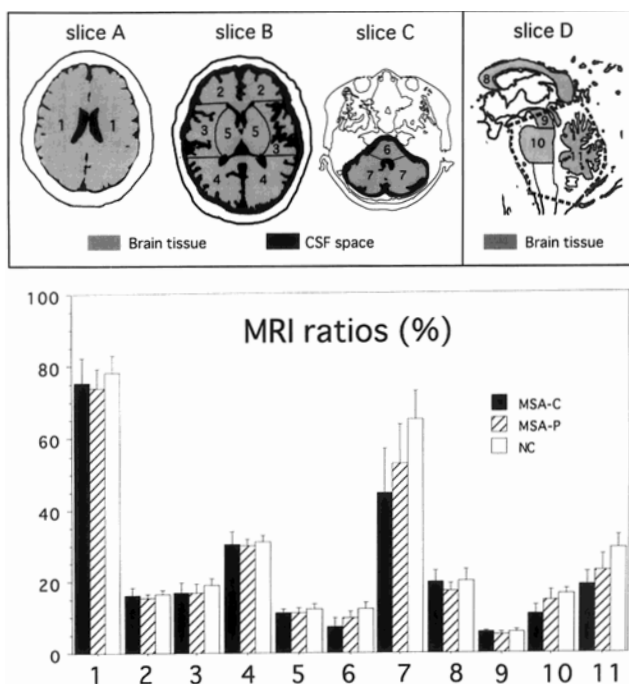


Fig. 2 The upper half of Fig. 2 shows square MRI measurements which were done at seven sites (1–7) in three axial slices (A,B,C) and at four sites (8–11) in a mid-sagittal slice (D). The boundary between region (2) and region (3) was the line through the most anterior point of the anterior horn in the lateral ventricle (slice B). The boundary between region (3) and region (4) was the line at the most posterior point of the thalamus (slice B). The boundary between region (3) and region (5) was the line that joined the outermost edges of the caudate nucleus (head), the putamen, and the thalamus (slice B). The pontine area (6) included the area of the middle cerebellar peduncle (slice C). The lower margin of the midbrain (9) was a line drawn perpendicular to the long axis of the pons, at the junction of the ventral portions of the midbrain and the pons (slice D). The lower margin of the pons (10) was a line drawn perpendicular to the long axis of the pons, at the junction of the ventral portions of the pons and the medulla (slice D). The dotted line indicates the outermost edge of the posterior fossa (slice D). The lower half of Fig. 2 shows the mean and SD of the MRI area ratio for regions (1) – (11).

cerebral area in slice B, (3) perisylvian cerebral area in slice B, (4) posterior cerebral area in slice B, (5) deep cerebral gray matter in slice B, (6) pons in slice C, (7) cerebellum in slice C, (8) corpus callosum in slice D, (9) midbrain in slice D, (10) pons in slice D, and (11) cerebellum in slice D. To compensate for individual variation in head size, we measured a reference area as a standard for the regions of interest. As a reference area, we measured the total area of the cranial fossa (TCF) in slice A and slice B, and the total area of the posterior fossa (TPF) in slice C and slice D. The TCF in two axial slices (A, B) was used to standardize regions (1)–(5). The TPF in axial and midsagittal slices (C, D) was used to standardize regions (6)–(11). The MRI area ratio was calculated as the area of each region from (1) to (5) divided by that of the TCF and as the area of each region from (6) to (11) divided by that of the TPF, according to the method previously described [13, 14, 23].

Data on ERPs and MRI area ratios were measured independently by different data analysts. The analysts of ERPs were not given access to the data of the analysts of MRI area ratios, and vice versa.

Statistical analysis

Statistical analysis was performed using a Stat View J–5.0 computer program (SAS Institute Inc). We used a one-way ANOVA test for com-

parison of the mean values of quantitative ERP and MRI measurements among the MSA-C, MSA-P, and NC groups. We used Pearson's correlation coefficient (r) in MSA, to evaluate the relationship between ERP and MRI and between ERP and duration of illness. When r was 0.50 or more, the correlation was regarded as significant.

Results

ERP data

All of the normal subjects and the MSA patients could perform the task at an error rate not exceeding 5%. Grand mean ERP waveforms during the task were obtained from midline electrodes (Fig. 3). The mean and SD of the ERP values and reaction time in MSA-C, MSA-P, and NC subjects are shown in Fig. 4. The P3a peak was more frequently undetectable in the MSA-C and MSA-P groups than in the NC group; P3a peaks were undetectable in 6/15 MSA-C patients (40%), in 8/12 MSA-P patients (67%), and in 2/21 NC subjects (9.5%). One-way ANOVA was used to determine the statistical differences of ERP and reaction time values among the MSA-C, MSA-P, and NC groups. Dunnett and Bonferroni/Dunn tests were further applied to N1 latency, N2 latency, P3b latency, P3b amplitude, P3a amplitude, and reaction time. No significant changes were seen in N1 or N2 latency to either rare targets or rare nontargets, in either MSA-C or MSA-P, compared with the normal control group. Significant difference was found for P3a amplitude and reaction time in both MSA-C and MSA-P group, compared with the normal control group (Table 2). Significant difference was found for P3b latency and P3b amplitude in MSA-C but not in MSA-P, compared with normal control group (Table 2).

MRI findings

As shown in Table 1, abnormal intensity in the putamen was found in 8/15 MSA-C patients (53%) and in 11/12

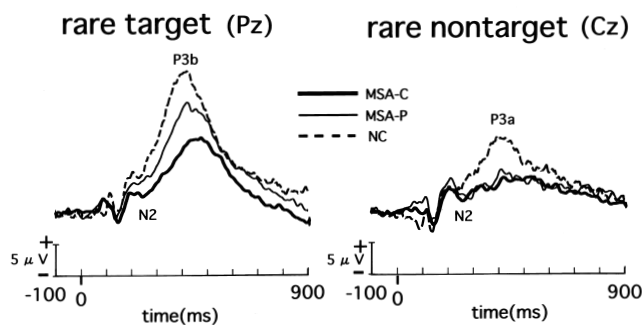


Fig. 3 Grand mean waveforms of visual ERPs in MSA-C (thick solid line), MSA-P (thin solid line), and NC subjects (dotted line). Upward deflection of the tracing indicates positive activity. P3b latency after rare target stimuli was delayed in MSA-C. P3a and P3b amplitudes were reduced in both MSA-C and MSA-P.

MSA-P patients (92%). The “cross sign” in the pons was found in all MSA-C patients and in 10/12 MSA-P patients (83%). Atrophy of the pons or the cerebellum was

seen in all MSA-C patients and in 9/12 MSA-P patients (75%).

The mean and SD of the MRI area ratios at 11 sites in MSA-C, MSA-P, and NC subjects are shown in Fig. 2. One-way ANOVA was used to determine the statistical differences of MRI area ratios among MSA-C, MSA-P, and NC groups. Dunnett and Bonferroni/Dunn tests were applied to the 11 MRI ratios. Significant difference was found only for the perisylvian cerebral area (slice B), the deep cerebral gray matter (slice B), the pons (slices C and D), the cerebellum (slices C and D), and for the corpus callosum (slice D) (Table 2).

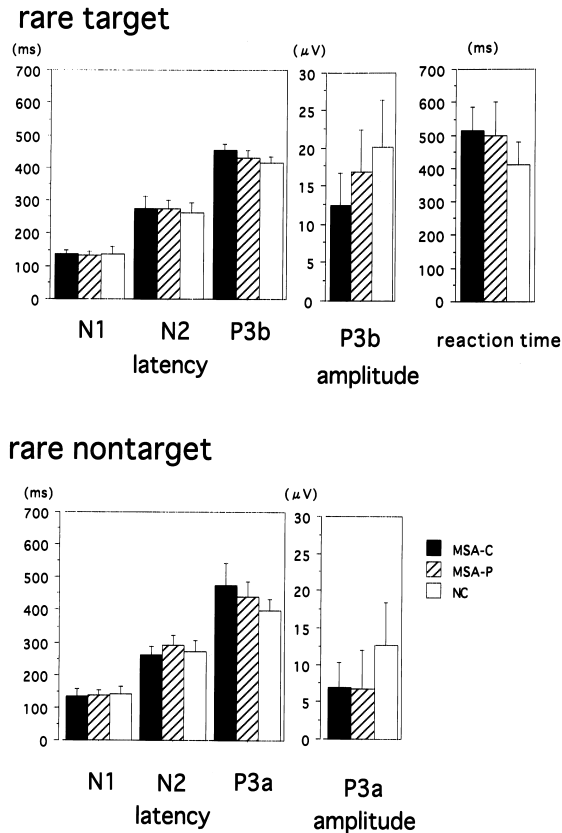


Fig. 4 The upper half of Fig. 4 shows the mean and SD of ERP latency and amplitude and reaction time for rare target stimuli in MSA-C, MSA-P, and NC subjects. The lower half of Fig. 4 shows the mean and SD of ERP latency and amplitude for rare nontarget stimuli in MSA-C, MSA-P, and NC subjects.

Correlation of ERP findings to duration of illness and MRI area ratios

As shown in Table 3, Pearson’s correlation coefficient was used in MSA-C and MSA-P subjects, to analyse the correlation of P3b latency to duration of illness and MRI area ratios for 5 sites: the perisylvian cerebral area (slice B), the deep cerebral gray matter (slice B), the corpus callosum (slice D), the pons (slice D), and the cerebellum (slice D). In MSA-C, P3b latency was significantly correlated with duration of illness and MRI area ratios for the pons, and the cerebellum. In MSA-P, P3b latency was significantly correlated with MRI area ratios for the corpus callosum, the pons, and the cerebellum. Pearson’s correlation coefficient was also used for the whole MSA group (15 MSA-C and 12 MSA-P subjects), to analyse the correlation of P3b latency to duration of illness and MRI area ratios for the 5 sites. P3b latency was significantly correlated with MRI area ratios for the pons and the cerebellum.

Table 2 Analysis of variance in ERP and MRI data

	one way ANOVA	Dunnett		Bonferroni/Dunn		
	MSA-C MSA-P NC	MSA-C vs NC	MSA-P vs NC	MSA-C vs NC	MSA-P vs NC	MSA-C vs MSA-P
ERP						
P3b latency	F = 14.6****	✓		****		**
P3b amplitude	F = 6.3**	✓		***		
P3a amplitude	F = 7.4**	✓	✓	**	**	
reaction time	F = 7.3**	✓	✓	***	**	
MRI measurements						
(3) perisylvian cerebral area	F = 3.3*	✓	✓			
(5) deep cerebral gray matter	F = 3.4*	✓	✓			
(6) pons	F = 22.4****	✓	✓	****	**	**
(7) cerebellum	F = 14.6****	✓	✓	****	**	**
(8) corpus callosum	F = 4.3*	✓	✓		**	
(10) pons	F = 27.5****	✓		****		****
(11) cerebellum	F = 26.9****	✓	✓	****	****	

The numbers, (3), (5)–(8), (10), (11) correspond to numbers in Fig 2.

✓ significant difference

* p < 0.05; ** p < 0.01; *** p < 0.001; **** p < 0.0001

Table 3 Correlation of P3b latency to other factors in MSA-C, MSA-P, and the whole MSA group

	MSA-C (n = 15)	MSA-P (n = 12)	MSA (n = 27)
duration of illness	$r = 0.778$ ($p = 0.001$)	ns	ns
(3) perisylvian cerebral area	ns	ns	ns
(5) deep cerebral gray matter	ns	ns	ns
(8) corpus callosum	ns	$r = -0.733$ ($p = 0.0046$)	ns
(10) pons	$r = -0.714$ ($p = 0.0046$)	$r = -0.635$ ($p = 0.0244$)	$r = -0.766$ ($p < 0.0001$)
(11) cerebellum	$r = -0.663$ ($p = 0.0117$)	$r = -0.661$ ($p = 0.0171$)	$r = -0.717$ ($p < 0.0001$)

The numbers, (3), (5), (8), (10), (11) correspond to numbers in Fig 2.
ns not significant

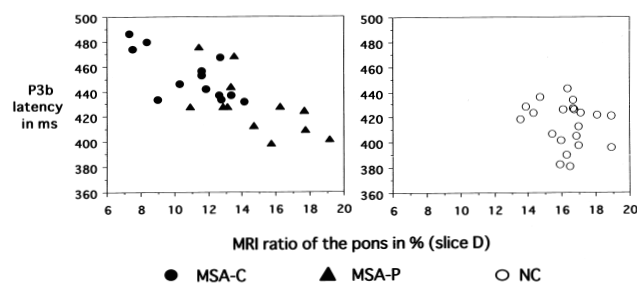


Fig. 5 Scattergrams of the P3b latency after rare targets versus MRI area ratio of the pons [region (10) in slice D]. The left half of this figure shows scattergrams of P3b latency (Pz) versus the MRI area ratio of the pons for MSA-C (closed circles) and MSA-P patients (closed triangles). The right half of this figure shows scattergrams of P3b latency (Pz) versus the MRI area ratio of the pons for NC subjects (open circles)

Discussion

We employed the same task which we have used in past studies on ERP waveforms recorded from 32 scalp electrodes in normal subjects [30] and on ERP changes in Parkinson's disease and other parkinsonian syndromes [25, 26]. N1 was measured at Oz, since we observed N1 with enhanced negativity to rare targets at the posterior scalp sites [30]. P3a was typically larger in amplitude than P3b over the frontal and central electrode sites [2, 9]. We observed P3a with enhanced positivity to rare nontargets at the frontal and vertex sites and P3b with enhanced positivity to rare targets at the parietal sites [30]. Therefore, P3a and P3b were defined as P3 potentials measured at Cz after rare nontargets and at Pz after rare targets, respectively.

The purpose of our study was to clarify whether visual ERP abnormalities exist or not in two MSA subtypes. As shown in Table 2, visual ERP results found common to MSA-C and MSA-P, compared with NC subjects, were 1) normal N1 and N2 components to rare targets and rare nontargets, 2) frequently undetectable P3a

peaks to rare nontargets, 3) significant P3a amplitude reduction to rare nontargets, and 4) significantly prolonged reaction time to rare targets. Visual ERP results found in MSA-C but not in MSA-P, compared with NC subjects, were 1) P3b latency delay to rare targets and 2) P3b amplitude reduction to rare targets. P3b latency in MSA-C was significantly longer than in MSA-P.

In previous studies, P3b latency prolongation was found among 10 OPCA patients during an auditory odd-ball task [12] and attenuated visual P3a [26] was the only change found in 9 SND patients. These results are consistent with our present study. N1 as an early auditory ERP component is thought to reflect normal attention process [15, 18]. In the missing stimulus paradigm [19, 20] the maximum amplitude was found in the preoccipital region, for N2 associated with omitted flashes. Therefore, N2 was assumed to reflect a decision process related to sensory discrimination of attended stimuli. It is considered that P3a reflects automatic cognitive processing and indicates the early cortical response to an incoming signal [10, 17, 30]. It is also considered that P3b reflects controlled cognitive processing and indexes the attentional and memory-related operations involved in the processing of that signal [10, 17, 30].

The ERP results in our study suggest that an early stage of the visual information process related to N1 and a visual discrimination process related to N2 might be preserved in both MSA-C and MSA-P. The P3a amplitude attenuation in both MSA-C and MSA-P suggest an impaired synchronous activity of neural generators related to automatic cognitive processing during the visual discrimination process. The P3b abnormality found only in the MSA-C group suggests the impairment of the controlled cognitive processing after visual discrimination process in this group.

Previous MRI studies on quantitative square measurements revealed atrophy of the putamen, the pons, and the cerebellum in axial and sagittal planes in OPCA and SND [23, 24, 29]. Recently, the existence of cerebral atrophy was revealed on quantitative MRI measurements in MSA [7]. As shown in Table 2, MRI results found common to MSA-C and MSA-P, as compared to NC subjects, were reduced MRI ratios in the perisylvian cerebral area, the deep cerebral gray matter, the pons, and the cerebellum. Reduced MRI ratio of the corpus callosum was found in MSA-P but not in MSA-C, as compared with NC subjects. The MRI ratio of the pons in MSA-C was significantly smaller than in MSA-P.

In the MSA-C group with significantly prolonged P3b latency, P3b latency was significantly correlated not only with pontine and cerebellar MRI ratios but also with duration of illness. Therefore, we believe that the correlation between P3b latency and pontine and cerebellar MRI ratios does not directly prove but strongly suggests the correlation between P3b latency and ponto-cerebellar degeneration. Even in the MSA-P group without sig-

nificant P3b latency changes, P3b latency was significantly correlated with MRI ratios for the pons and the cerebellum. We further confirmed that P3b latency in the whole MSA group (MSA-C and MSA-P) was significantly correlated with MRI ratios for the pons and the cerebellum. These results indicate that P3b latency changes in parallel with pontocerebellar degeneration in both MSA-C and MSA-P. In our previous study [8] on 22 patients with nondemented Parkinson's Disease, we

could not find significant association between P3b latency and any MRI ratio changes. Accordingly, the significant associations in MSA between P3b latency and MRI ratio are likely to be the result specific to MSA.

■ **Acknowledgments** This study was supported in part by the Research Committee of Ataxic Diseases, The Ministry Health and Welfare of Japan (Chairman; Prof. I. Kanazawa, Univ. of Tokyo). We thank Ryosuke Ushijima and Hiroyasu Shinozuka for technical support in ERP measurements.

References

- Berent S, Giordani B, Gilman S, Junck L, Lehtinen S, Markel DS, Boivin M, Kluin KJ, Parks R, Koeppe RA (1990) Neuropsychological changes in olivopontocerebellar atrophy. *Arch Neurol* 47: 997–1001
- Courchesne E, Hillyard S, Galambos R (1975) Stimulus novelty, task relevance, and the visual evoked potential in man. *Electroencephalogr Clin Neurophysiol* 39: 131–143
- Gilman S, Low PA, Quinn N, Albanese A, Ben Shlomo Y, Fowler CJ, Kaufmann H, Klockgether T, Lang AE, Lantos PL, Litvan I, Mathias CJ, Oliver E, Robertson D, Schatz I, Wenning GK (1999) Consensus statement on the diagnosis of multiple system atrophy. *J Neurol Sci* 163: 94–98
- Hasegawa K (1983) The clinical assessment of dementia in the aged: a dementia screening scale for psychogeriatric patients. In: Burgener M, Lehr U, Lang E (ed) *Aging in the eighties and beyond*. Springer, New York, pp 207–218
- Hirayama K, Takayanagi T, Nakamura R, Yanagisawa N, Hattori T, Kita K, Yanagimoto Y, Fujita S, Nagaoka M, Satomura M, et al. (1994) Spinocerebellar degenerations in Japan: a nationwide epidemiological and clinical study. *Acta Neurol Scand Suppl* 153: 1–22
- Hirono N, Yamadori A, Kameyama M, Mezaki T, Abe K (1991) Spinocerebellar degeneration (SCD): cognitive disturbances. *Acta Neurol Scand* 84: 226–230
- Horimoto Y, Aiba I, Yasuda T, Ohkawa Y, Katayama T, Yokokawa Y, Goto A, Ito Y (2000) Cerebral atrophy in multiple system atrophy by MRI. *J Neurol Sci* 173: 109–112
- Kamitani T, Kuroiwa Y, Wang L, Li M, Ushijima R, Shinozuka H, Takahashi T, Suzuki Y, Hasegawa O (1999) Visual P300 in extrapyramidal degenerative disorders. *Rinsho Noha (Clinical Encephalography)* 41: 356–365
- Knight RT (1984) Decreased response to novel stimuli after prefrontal lesions in man. *Electroencephalogr Clin Neurophysiol* 59: 9–20
- Lagopoulos J, Gorden E, Barhamali H, Lim CL, Li WM, Clouston P, Morris JG (1998) Dysfunctions of automatic (P300a) and controlled (P300b) processing in Parkinson's disease. *Neurol Res* 20: 5–10
- Meco G, Gasparini M, Doricchi F (1996) Attentional functions in multiple system atrophy and Parkinson's disease. *J Neurol Neurosurg Psychiatry* 60: 393–398
- Mochizuki Y, Oishi M, Hara M, Takasu T (1997) P300 and cerebral blood flow before and after TRH in olivopontocerebellar atrophy. *Int. J Neurosci* 92: 119–126
- Nabatame H, Fukuyama H, Akiguchi I, Kameyama M, Nishimura K, Nakano Y (1988) Spinocerebellar degeneration: qualitative and quantitative MR analysis of atrophy. *J Comput Assist Tomogr* 12: 298–303
- Onodera O, Idezuka J, Igarashi S, Takiyama Y, Endo K, Takano H, Oyake M, Tanaka H, Inuzuka T, Hayashi T, Yuasa T, Ito J, Miyatake T, Tsuji S (1998) Progressive atrophy of cerebellum and brainstem as a function of age and the size of the expanded CAG repeats in the MJD1 gene in Machado-Joseph disease. *Ann Neurol* 43: 288–296
- Picton TW, Hillyard SA (1974) Human auditory evoked potentials. II. Effects of attention. *Electroencephalogr Clin Neurophysiol* 36: 191–199
- Pillon B, Dubois B, Agid Y (1996) Testing cognition may contribute to the diagnosis of movement disorders. *Neurology* 46: 329–334
- Polich J (1998) P300 clinical utility and control of variability. *J Clin Neurophysiol* 15: 14–33
- Polich J, Ladish C, Bloom FE (1990) P300 assessment of early Alzheimer's disease. *Electroencephalogr Clin Neurophysiol* 77: 179–189
- Ritter W (1979) A brain event-related to the making of a sensory discrimination. *Science* 203: 1358–1361
- Ritter W, Simson R, Vaughan HG Jr, Macht M (1982) Manipulation of event-related potentials manifestation of information processing stage. *Science* 218: 909–911
- Robbins TW, James M, Lange KW, Owen AM, Quinn NP, Marsden CD (1992) Cognitive performance in multiple system atrophy. *Brain* 115: 271–291
- Robbins TW, James M, Owen AM, Lange KW, Lees AJ, Leigh PN, Marsden CD, Quinn NP, Summers BA (1994) Cognitive deficits in progressive supranuclear palsy, Parkinson's disease, and multiple system atrophy in tests sensitive to frontal lobe dysfunction. *J Neurol Neurosurg Psychiatry* 57: 79–88
- Schulz JB, Klockgether T, Petersen D, Jauch M, Muller Schauenburg W, Spieker S, Voigt K, Dichgans J (1994) Multiple system atrophy: natural history, MRI morphology, and dopamine receptor imaging with 123IBZM-SPECT. *J Neurol Neurosurg Psychiatry* 57: 1047–1056
- Wakai M, Kume A, Takahashi A, Ando T, Hashizume Y (1994) A study of parkinsonism in multiple system atrophy: clinical and MRI correlation. *Acta Neurol Scand* 90: 225–231
- Wang L, Kuroiwa Y, Kamitani T (1999) Visual event-related potential changes at two different tasks in nondemented Parkinson's disease. *J Neurol Sci* 164: 139–147
- Wang L, Kuroiwa Y, Kamitani T, Li M, Takahashi T, Suzuki Y, Shimamura M, Hasegawa O (2000) Visual event-related potentials in progressive supranuclear palsy, corticobasal degeneration, striatonigral degeneration, and Parkinson's disease. *J Neurol* 247: 356–363

-
27. Wenning GK, Ben-Shlomo Y, Hughes A, Daniel SE, Lees A, Quinn NP (2000) What clinical features are most useful to distinguish definite multiple system atrophy from Parkinson's disease? *J Neurol Neurosurg Psychiatry* 68: 434–440
 28. Wenning GK, Tison F, Ben Shlomo Y, Daniel SE, Quinn NP (1997) Multiple system atrophy: a review of 203 pathologically proven cases. *Mov Disord* 12: 133–147
 29. Yagishita T, Kojima S, Hirayama K (1995) MRI study of degenerative process in multiple system atrophy. *Rinsho Shinkeigaku* 35: 126–131
 30. Yamazaki T, Kamijo K, Kenmochi A, Fukuzumi S, Kinuya T, Takaki Y, Kuroiwa Y (2000) Multiple equivalent current dipole source localization of event-related potentials during odd-ball paradigm with motor response. *Brain topography* 12: 159–175